David W. Scoville,[1] Holly A. Cyphert,[2] Lan Liao,[3] Jianming Xu,[3] Al Reynolds,[4] Shuangli Guo,[2] and Roland Stein[1,2]

MLL3 and MLL4 Methyltransferases Bind to the MAFA and MAFB Transcription Factors to Regulate Islet β-Cell Function

Diabetes 2015;64:3772–3783 | DOI: 10.2337/db15-0281

Insulin produced by islet β-cells plays a critical role in glucose homeostasis, with type 1 and type 2 diabetes both resulting from inactivation and/or loss of this cell population. Islet-enriched transcription factors regulate β-cell formation and function, yet little is known about the molecules recruited to mediate control. An unbiased in-cell biochemical and mass spectrometry strategy was used to isolate MafA transcription factor–binding proteins. Among the many coregulators identified were all of the subunits of the mixed-lineage leukemia 3 (Mll3) and 4 (Mll4) complexes, with histone 3 lysine 4 methyltransferases strongly associated with gene activation. MafA was bound to the ∼1.5 MDa Mll3 and Mll4 complexes in size-fractionated β-cell extracts. Likewise, closely related human MAFB, which is important to β-cell formation and coproduced with MAFA in adult human islet β-cells, bound MLL3 and MLL4 complexes. Knockdown of NCOA6, a core subunit of these methyltransferases, reduced expression of a subset of MAFA and MAFB target genes in mouse and human β-cell lines. In contrast, a broader effect on MafA/MafB gene activation was observed in mice lacking NCoA6 in islet β-cells. We propose that MLL3 and MLL4 are broadly required for controlling MAFA and MAFB transactivation during development and postnatally.

Diabetes mellitus is a disease that affects the body's ability to maintain euglycemia, with type 1 characterized by a loss of insulin-producing islet β-cells and type 2 (T2DM) by peripheral insulin resistance and β-cell dysfunction. One proposed treatment for type 1 diabetes is to replace diseased β-cells with those generated from human embryonic stem cells (hESCs) or induced pluripotent stem cells (1). The principal limitation in producing functional β-cells has been directing the final postnatal maturation steps (2), which involves expression of proteins required for glucose sensitivity and insulin secretion (3).

Islet-enriched transcription factors are essential for embryonic formation and postnatal function of β-cells (4–6). For example, very early exocrine and endocrine pancreatic development is driven by Pdx-1 starting at embryonic day 8.5 (e8.5) in mice, with mice and humans both lacking a functional copy suffering from pancreatic agenesis (4,5). In contrast, Ngn3 expressed from e9.5 is only required in the formation of endocrine cell types (i.e., β, α [hormone glucagon producing], δ [somatostatin], ε [ghrelin], and pancreatic polypeptide) (6). MafA is expressed even later during development and only in β-cells (i.e., e13.5), contributing in postnatal maturation steps (7). Interestingly, the induction of glucose-sensitive insulin secretion in vivo from transplanted hESC-derived endocrine progenitors correlates with MAFA expression (8). Moreover, the production of only Pdx-1, Ngn3, and MafA is sufficient to reprogram mouse exocrine, intestinal, and liver cells into insulin$^+$ β-like cells in vivo (9–11). Although these examples clearly illustrate the fundamental importance of islet-enriched activators to β-cells, the transcriptional mechanisms involved are not well defined.

[1]Department of Cell and Developmental Biology, Vanderbilt University School of Medicine, Nashville, TN
[2]Department of Molecular Physiology and Biophysics, Vanderbilt University School of Medicine, Nashville, TN
[3]Department of Molecular and Cellular Biology, Baylor College of Medicine, Houston, TX
[4]Department of Cancer Biology, Vanderbilt University School of Medicine, Nashville, TN

Corresponding author: Roland Stein, roland.stein@vanderbilt.edu.

Received 27 February 2015 and accepted 3 July 2015.

This article contains Supplementary Data online at http://diabetes.diabetesjournals.org/lookup/suppl/doi:10.2337/db15-0281/-/DC1.

Transcription factors primarily regulate gene activation by recruitment of coregulators, which often influence expression by directly binding to the basal transcriptional machinery and/or through epigenetic remodeling of the chromatin structure. These coregulators can have positive (coactivator) and negative (corepressor) actions on target gene transcription (12), thus conferring a second level of specificity to the transcriptional response. Coregulator recruitment is, in turn, controlled by the spatial and temporal expression patterns and posttranslational modifications of the transcription factor and/or coregulator. Unfortunately, little is known about the coregulators recruited by islet-enriched transcription factors. Although there are hundreds of known coregulators (http://www.nursa.org/), such knowledge is limited to candidate studies linking, for example, Pdx-1 to p300 (13), Set7/9 (14), HDAC1/2 (15), PCIF1 (16), and Bridge-1 (17). In contrast, MafA has only been linked to p/CAF (18).

In this study, we used an "in cell" reversible cross-link immunoprecipitation (Re-CLIP) and mass spectrometry (MS) approach to isolate coregulators of MafA from mouse β-cells. Notably, all nine subunits of the Mll3 and Mll4 histone 3 lysine 4 (H3K4) methyltransferase complexes were identified in the MafA immunoprecipitates, but none of the unique subunits of the other mammalian Mll complexes were detected (e.g., Menin, Mll1, Mll2 of Mll1/2 complexes; Set1A, Set1B, Wdr82 in Set1A/B complexes). (Mll3 and Mll4 will be referred to as Mll3/4 for simplicity.) These methyltransferases were also found to bind MAFB, a closely related transcription factor essential to mouse β-cell development and coexpressed with MAFA in adult human islets (19,20). Notably, mouse islet β-cell function is compromised in a heterozygous null mutant of NCoA6, a key subunit of Mll3/4 (21). Decreased NCOA6 levels reduced expression of a subset of MAFA- and MAFB-regulated genes in human and rodent β-cell lines, with evidence provided that this results from limiting gene transcriptional start site (TSS) H3K4 trimethylation. Interestingly, there is essentially complete overlap of MafA and Mll3/4 transcriptional control in islets isolated after embryonic β-cell–specific removal of NCoA6 or MafA in vivo. These results suggest that MLL3/4 coactivator recruitment by MAFA and MAFB is important to the formation and adult function of islet β-cells.

RESEARCH DESIGN AND METHODS

Cell Culture and Immunoblotting Analysis

Mouse βTC-3 cells were maintained in DMEM containing 25 mmol/L glucose, 10% FBS, and 100 units/mL penicillin/streptomycin (22). Human EndoC-βH1 (23) cells were grown in DMEM containing 5.6 mmol/L glucose, 2% BSA, 50 μmol/L 2-mercaptoethanol, 10 mmol/L nicotinamide, 5.5 μg/mL transferrin, 6.7 ng/mL selenite, 100 units/mL penicillin, and 100 units/mL streptomycin. βTC-3 cells were infected with an adenovirus overexpressing GFP alone or a Flag-tagged MafA (provided by Dr. Qiao Zhou, Harvard University) at a multiplicity of infection of 200 under conditions described previously (24). Nuclear extract was prepared 48 h postinfection as described below. Primary antibodies for immunoblotting (25) are listed in Supplementary Table 1. Horseradish peroxidase–conjugated anti-rabbit, anti-mouse, or anti-goat secondary antibody was used at 1:2000 (Promega). Immunoblots were quantitated with ImageJ software (National Institutes of Health).

Re-CLIP and Immunoprecipitation Assays

The Re-CLIP protocol was adapted from Smith et al. (26). Briefly, ~10^9 βTC-3 cells were cross-linked using 0.1 mmol/L dithiobis (succinimidyl propionate) (DSP) in PBS for 30 min at 37°C. Cells were then harvested and nuclear extract was prepared by high salt (400 mmol/L NaCl) extraction (25). Magnetic protein G beads (Life Technologies) were covalently cross-linked with MafA antibody (20 μg) and were preincubated with an MafA-blocking peptide (^{32}KKEPPEAERFC^{42}, 100-fold excess antibody) or with PBS alone. Extract and beads were incubated for 3 h at 4°C, washed with radioimmunoprecipitation (RIPA) buffer (10 mmol/L Tris, pH = 8.0, 140 mmol/L NaCl, 0.5% Triton X-100, 1% sodium deoxycholate, 0.1% SDS), and eluted in RIPA supplemented with 200 mmol/L dithiothreitol (DTT). The eluted proteins were visualized by PAGE/silver staining, and protein identification was determined by liquid chromatography–tandem MS (LC/MS/MS) or Multidimensional Protein Identification Technology (MudPIT) analysis in the Vanderbilt University Proteomics Core. Immunoprecipitation experiments were performed with the antibodies listed in Supplementary Table 1 at 10 μg each, as described above for Re-CLIP, omitting the DSP step and substituting PBS for RIPA.

Sucrose Gradient Ultracentrifugation and Electrophoretic Mobility Shift Assays

Sucrose gradients were performed as described earlier (25). Briefly, βTC-3 nuclear extract (600–1000 μg) was collected by high salt extraction (25) and separated over a 5–35% sucrose gradient (4.5 mL total volume). Fractions (300 μL each, excluding the first 500 μL) were analyzed by immunoblotting, rat *insulin II* C1 element gel shift (25), and immunoprecipitation analysis. HeLa cells were transfected with expression plasmids encoding human MAFA and/or MAFB (25). Antibodies used for gel shift are listed in Supplementary Table 1.

Small Interfering RNA Treatment of β-Cell Lines

Knockdown in βTC-3 and EndoC-βH1 cells was achieved using ON-TARGETplus small interfering (si)RNAs of mouse MafA (#J-041353–09), mouse NCoA6 (#J-041129–6), human MAFA (#L-027343–01), human MAFB (#L-009018–00), and human NCOA6 (#L-019107–00). The targeting siRNA (0.5 nmol) or a nontargeting control (#D001810; GE Healthcare Dharmacon) was introduced into βTC-3 cells (4×10^6) using Buffer V (Lonza #VVCA-1003) with an Amaxa Nucleofector 2 (Program G-016; Lonza, Walkersville, MD). EndoC-βH1 cells (2×10^6) were transfected with siRNAs (50 pmol/L) using the Dharmafect #1 reagent (GE

Healthcare Dharmacon #T-2001), following the manufacturer's protocol. Nuclear extract, RNA, and chromatin were collected 72 h after transfection.

Quantitative PCR and Qiagen RT^2 Profiler PCR Array Analysis

RNA was collected from βTC-3 cells using the RNeasy kit (Qiagen). The Trizol reagent (Life Technologies) and the DNA-Free RNA Kit (Zymo Research) were used for EndoC-βH1 cells and mouse islets. The iScript cDNA synthesis kit (Bio-Rad Laboratories, Inc.) was used for cDNA synthesis. The quantitative (q)PCR reactions were performed with the gene primers listed in Supplementary Table 2 on a LightCycler 480 II (Roche), and analyzed by the ΔΔCT method (27). Significance was calculated by comparing the ΔCT values in all but Fig. 7*A* and *B*, wherein each mutant was normalized to a control littermate. The Qiagen RT^2 Profiler PCR array for human diabetes genes (Cat. No. 330231 PAHS-023ZA) was screened with 1 ng cDNA from EndoC-βH1 cells, following the manufacturer's guidelines.

Chromatin Immunoprecipitation

Chromatin was prepared from βTC-3 cells and EndoC-βH1 cells by cross-linking for 10 min with 1% formaldehyde, followed by lysis in buffer containing 1% NP-40. The centrifuged pelleted nuclei were lysed in SDS buffer (50 mmol/L Tris, 10 mmol/L EDTA, 1% SDS), and chromatin was sonicated using a Diagenode Bioruptor. DNA (10 μg) was incubated with 5 μg of antibody or species-matched IgG, and chromatin immunoprecipitation (ChIP) was performed as described previously (28). Antibodies are listed in Supplementary Table 1, and the qPCR primers used for the analysis are listed in Supplementary Table 2.

Mouse Lines, Intraperitoneal Glucose Tolerance Test, and Islet Isolation

Floxed (fl) *MafA* (19) or *NCoA6* (29) mice were crossed with rat *insulin* II promoter-driven Cre (RIP-Cre) (30) transgenic mice to delete *MafA* (termed $MafA^{\Delta\beta}$) or *NCoA6* ($NCoA6^{\Delta\beta}$) specifically in β-cells. All mice were maintained on a mixed background (C57BL/6J, I129, Balb/c, 129S6/SvEvTac, FVB/N), although $MafA^{\Delta\beta}$ mice were mostly C57BL/6J. $MafA^{\Delta\beta}$, $NCoA6^{\Delta\beta}$, $MafA^{fl/fl}$ and/or $NCoA6^{fl/fl}$ mice were fasted for 6 h in the morning before the intraperitoneal glucose tolerance test. There was no change in total body weight in $MafA^{\Delta\beta}$ or $NCoA6^{\Delta\beta}$ mice (Supplementary Fig. 2*A*). Blood glucose levels were measured before (time 0) and then 15, 30, 60, and 120 min after an intraperitoneal injection of glucose (2 mg/g body weight) prepared in sterile PBS (20% w/v). Islets from 8-week-old mice were isolated using collagenase P (Roche) digestion and hand picking (31). The Vanderbilt University Institutional Care and Use Committee approved all of these studies.

Tissue Collection and Immunofluorescence

Pancreata were dissected and fixed in 4% paraformaldehyde in PBS for 4 h, followed by paraffin embedding (32). The entire e15.5 pancreas was serially sectioned (6 μm per section) and every 10th section analyzed by immunofluorescence. Three sections at least 120 μm apart were examined at 8 weeks for islet architecture and for Slc30a8 and Slc2a2 expression. The primary antibody list is provided in Supplementary Table 1. Species-matched secondary antibodies were used for immune detection at 1:1000 (Jackson ImmunoResearch Laboratories). Slides were mounted with Dapi Fluoromount-G (SouthernBiotech #0100-20) and images acquired on a Zeiss Axio Imager M2 widefield microscope with Apotome.

Glucose-Stimulated Insulin Secretion

EndoC-βH1 cells (2×10^6) were placed in medium containing low glucose (1.1 mmol/L) for 12–14 h. Low or high glucose (15.5 mmol/L) medium was then added for 1 h. Medium and cell lysates (lysis buffer: 20 mmol/L Tris, 1% Triton X-100, 10% glycerol, 137 mmol/L NaCl, 2 mmol/L EGTA, 1X protease inhibitor tablet [Roche Diagnostics]) were collected and analyzed for insulin content by the Vanderbilt Hormone Assay Core. Glucose-stimulated insulin secretion was performed with 8-week-old islets in the Vanderbilt Islet Procurement and Analysis Core. Briefly, islets were size matched, incubated overnight in 5.6 mmol/L glucose and then treated with 5.6 mmol/L or 16.7 mmol/L glucose for 1 h. The insulin content in the medium and cell lysate was analyzed. Insulin secretion capacity was calculated as media insulin over cell lysate insulin content. Glucose-stimulated levels are presented as the 15.5 mmol/L and 1.1 mmol/L values for EndoC-βH1 cells and 16.7 mmol/L glucose and 5.6 mmol/L glucose for isolated islets.

Statistics

Mean differences were tested for significance using a Student two-tailed *t* test. The minimal level of statistical significance is listed in the figure legend.

RESULTS

Identification of MafA Proteins Using Re-CLIP

MafA interacting proteins were isolated from mouse βTC-3 cells using a combined Re-CLIP/MS strategy (Fig. 1*A*) (26). The Re-CLIP procedure was selected over other isolation methods (e.g., tandem affinity purification [33]), because the dimerization, DNA binding, and activation capacity of MafA is regulated by many phosphorylation events (25). Amine-reactive DSP was used to covalently cross-link MafA to neighboring proteins, and MafA antibody was used to precipitate bound proteins. The signal-to-noise of the procedure was improved by using the MafA antibody blocked by MafA peptide in the control immunoprecipitation (as opposed to IgG) and by washing precipitated proteins with RIPA buffer. Bound proteins were eluted from MafA by the addition of DTT to cleave the disulfide bond in the cross-linker. As expected, Pdx-1 (22) and p/CAF (18), known MafA-interacting proteins, were bound to MafA after Re-CLIP (Fig. 1*B*). Moreover, many proteins were selectively bound to MafA in the immunoprecipitation conducted in the absence of blocking peptide (Fig. 1*C*).

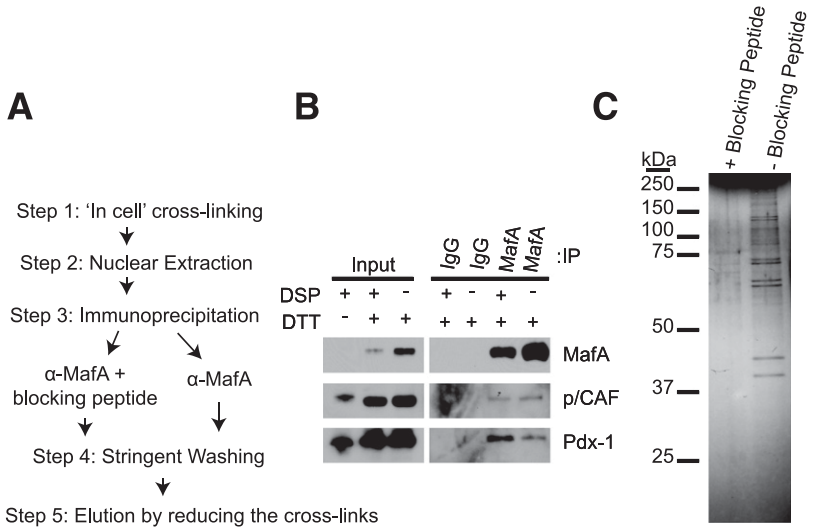

D

Protein	% Coverage	#Peptides from Control IP	# Peptides from MafA IP
Rbbp5	34	4	13
Ash2l	30	0	9
Wdr5	39	4	12
Dpy30	55	2	4
Utx	30	3	27
Ptip	10	0	6
NCoA6	2	1	3
Pa1	15	0	3
Mll4	4	1	3

Figure 1—MafA interacting proteins in β-cells were identified by Re-CLIP/MS. *A*: Schematic of the Re-CLIP protocol used for isolating MafA interacting proteins from mouse βTC-3 cells. DSP was the cross-linker used in step 1 and DTT was used to elute MafA cross-linked proteins in step 5. *B*: Immunoprecipitations performed with βTC-3 cells using control IgG or MafA antibody in the absence (−) or presence (+) of DSP treatment. The precipitate was then immunoblotted with MafA, p/CAF, and Pdx-1 antibodies. The input lanes contain ~1% of the nuclear extract; treatment with (+) DTT breaks the MafA-protein disulfide cross-link and returns MafA to its normal molecular weight. *C*: A representative image of proteins precipitated by MafA antibody preincubated with a blocking or scrambled control peptide after SDS-PAGE and silver staining. *D*: All of the proteins of the Mll4 complex were detected by Re-CLIP (IP); a representative MS result is shown. Mll3 was also present in the MudPIT analysis (Supplementary Table 3).

Numerous MafA bound proteins were detected upon MS analysis of the Re-CLIP products, with their activities consistent with a role in mediating MafA activity (Supplementary Table 3). It is notable that no other islet-enriched transcription factors or the p/CAF coactivator was identified by MS, presumably reflecting their relatively low abundance (e.g., Pdx-1, p/CAF) or inability to interact. This indicates that the results in Supplementary Table 3 represent only a portion of MafA-interacting proteins.

Our analysis focused on determining the significance of Mll3/4 coactivator binding to MafA because the evolutionary conserved COMPASS family of methyltransferases is strongly associated with gene activation due to their ability to mono-, di-, and trimethylate H3K4 within the enhancer and/or promoter region (34). MS identified all nine proteins of the ~1.5 MDa Mll4 complex (Fig. 1*D*), and Mll3 was additionally detected by the more sensitive MudPIT analysis (Supplementary Table 3). However, none of the unique COMPASS subunits of mammalian Mll1/2 (i.e., Mll1, Mll2, menin, Hcfc1/2, Psip1/2) or Set1A/B (i.e., Set1A, Set1B, Cfp1, Wdr82, Bod1, Bod1l) were detected. The ability of MafA to bind to Mll3/4 was also independently demonstrated in βTC-3 cells producing an adenovirus-driven Flag-tagged MafA (Supplementary Fig. 1).

MafA Comigrates With the High–Molecular Weight Mll3/4 Complexes Upon Sucrose Density Gradient Separation

βTC-3 nuclear proteins were separated by size in a 5–35% sucrose gradient to determine if the mobility of the ~90kDa MafA dimer was affected by interaction with Mll3/4. MafA was found in two distinct gradient size fractions. The faster mobility MafA, containing fractions 6–8, were surrounded by islet-enriched transcription factors of relatively low molecular weight (Fig. 2*A*) (Pdx-1, 31 kDa, fractions 3–5; Nkx6.1, 38 kDa, fractions 3–5; Hnf1α, 67 kDa, fractions 6–8; Nkx2.2, 30 kDa, fractions 3–5; Pax6, 50 kDa, fractions 6–8), whereas the high–molecular weight fraction 14 comigrated with the Rbbp5 (59 kDa), NCoA6 (220 kDa), Wdr5 (36 kDa), and Utx

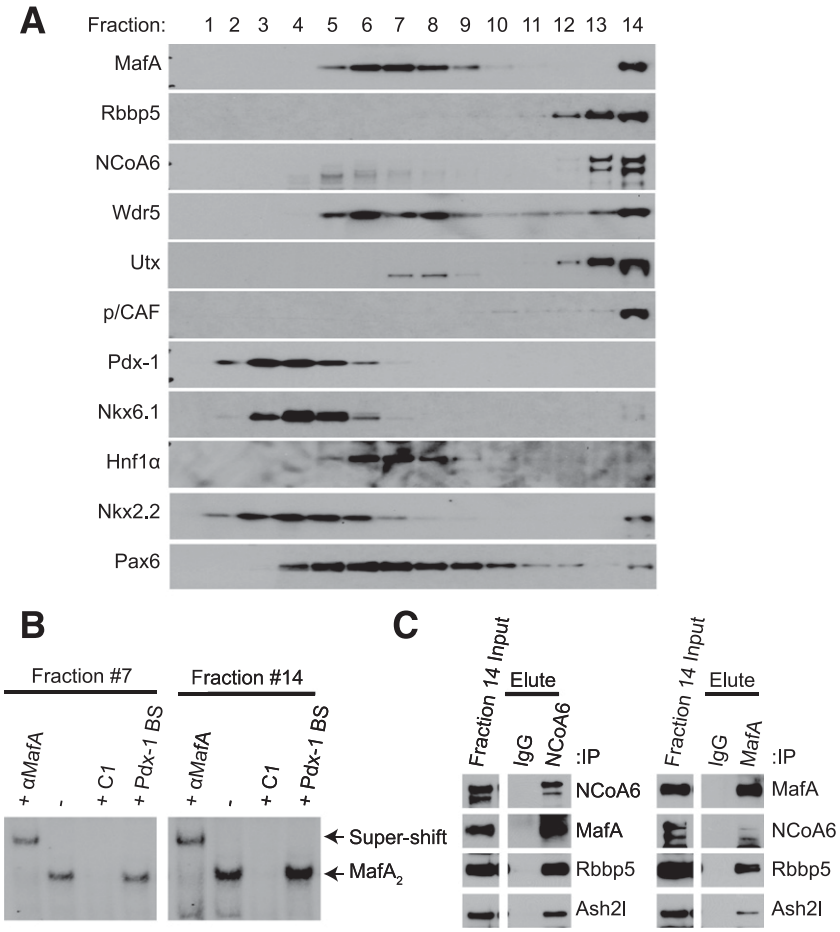

Figure 2—Sucrose gradient sedimentation reveals that MafA comigrates with the Mll3/4 complex. *A*: βTC-3 nuclear proteins were separated in a 5–35% sucrose gradient, and fractions were screened for MafA, Mll3/4 (i.e., Rbbp5, NCoA6, Wdr5, Utx), p/CAF, Pdx-1, Nkx6.1, Hnf1α, Nkx2.2, and Pax6 by immunoblotting. A significant portion of MafA was present in fraction 14, which contains Mll3/4 complexes. *B*: $MafA_2$ in fractions 7 and 14 binds specifically to the rat *insulin II* C1 enhancer element. MafA in these fractions was supershifted by anti-MafA antibody, while only unlabeled C1 and not an *insulin* Pdx-1 binding element (Pdx-1 BS) competed for binding. *C*: Immunoprecipitations (IP) performed on fraction 14 with antibody to NCoA6 (left) and MafA (right), which were then probed with MafA, NCoA6, Rbbp5, or Ash2l antibodies. The input lane contained ~5% of fraction 14.

(154 kDa) subunits of the Mll3/4 complex. In contrast, few other islet-enriched transcription factors were found in this high–molecular weight fraction. Antibody supershift and competitor analysis illustrated that the binding properties of MafA in fractions 7 and 14 were identical (Fig. 2*B*). In addition, immunoprecipitation experiments conducted with antibodies to NCoA6 or MafA demonstrated that MafA interacted with several Mll3/4 components in fraction 14 (Fig. 2*C*). These results strongly indicate that a significant fraction of MafA is associated with the Mll3/4 complex in β-cells.

A Subset of MafA-Regulated Genes Are Activated by the Mll3/4 Complexes in Mouse βTC-3 Cells

We next analyzed how Mll3/4 affected MafA activity by depleting MafA or NCoA6 from βTC-3 cells by siRNA-directed knockdown. The NCoA6 subunit lacks a DNA binding domain and is involved in recruiting Mll3/4 to a variety of transcription factors and nuclear receptors (35–38). Furthermore, Mll3 and Mll4 have redundant roles in the liver, and NCoA6 is required for activity of both methyltransferase complexes (36). Notably, mouse $NCoA6^{+/-}$ mutants have impaired glucose clearance (21), whereas overexpression of NCoA6 in rat INS-1 β-cells increases cell function (39). In addition, polymorphisms in *NCOA6* are associated with decreased human β-cell function (39). Our objective was to determine how closely Mll3/4 is linked to MafA-mediated transcriptional control.

MafA and NCoA6 protein levels in βTC-3 cells were both effectively (>80%) and specifically depleted by siRNA treatment (Fig. 3*A*). The effect of these conditions on expression of β-cell genes bound by MafA and downregulated in pancreas-specific deletion $MafA^{\Delta panc}$ mice was determined (40, 41) (Supplementary Table 4). As expected, the expression of most of these genes was decreased upon depletion of MafA (Fig. 3*B*; *Slc2a2*, *Ins2*, *Lifr*, *Prss53*, *Atp2a2*), but these conditions had no effect on *NCoA6* levels. In contrast, only a small subset of these

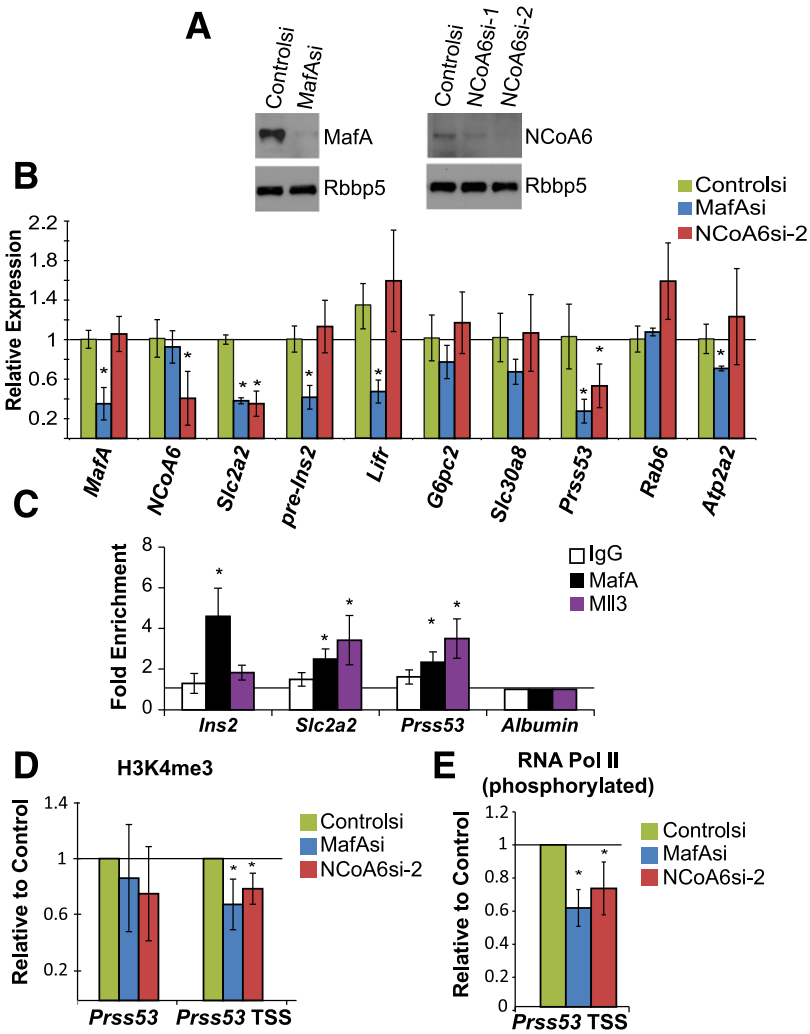

Figure 3—Knockdown of NCoA6 reduces MafA target gene expression in βTC-3 cells. Control siRNA (Controlsi) or siRNA specific to MafA (MafAsi) and NCoA6 (NCoA6si-1 and -2) was introduced into βTC-3 cells. *A*: MafA and NCoA6 were immunoblotted after corresponding depletion, with NCoA6si-2 most effective at reducing protein levels and used in all subsequent experiments. Rbbp5 levels were unaffected by siRNA treatment and served as a loading control. Densitometric analysis indicated effective knockdown of MafA (MafAsi = 0.04 ± 0.02 standard deviation) and NCoA6 (NCoA6si-2 = 0.16 ± 0.12). $n = 3$; *$P < 0.05$. *B*: NCoA6 affects expression levels of a subset of MafA-regulated genes in βTC-3 cells. mRNA expression was determined by qRT-PCR, normalized to *Gapdh* expression ($n = 3$–6). *C*: ChIP analysis reveals that MafA and Mll3 are bound to the same region of *Slc2a2* and *Prss53*. Fold enrichment was calculated using the percent input and normalized to background binding at the *Albumin* promoter ($n = 4$). *D*: H3K4 trimethylation levels were reduced near the TSS of *Prss53* in MafAsi- and NCoA6si-treated βTC-3 cells in ChIP analysis. The percentage input was calculated and normalized to Controlsi treated ($n = 3$). *E*: MafA and NCoA6 knockdown in βTC-3 cells decreased phosphorylated RNA polymerase (Pol) II binding to the TSS region of *Prss53* in ChIP assays ($n = 3$). All error bars indicate standard deviation. *$P < 0.05$.

MafA-activated genes was affected in the NCoA6 knockdown (i.e., *Slc2a2*, *Prss53*). This outcome was considered likely because a number of other potential MafA coregulators were identified here and previously (e.g., p/CAF (18) (Supplementary Table 1), although it is possible that some fraction of Mll3/4 activity is independent of NCoA6. In addition, ChIP analysis showed that Mll3 and MafA were bound within the same control regions of the *Slc2a2* and *Prss53* genes (Fig. 3*C*). Moreover, H3K4 trimethylation and elongating carboxy terminal tail phosphorylated RNA polymerase II levels were significantly reduced within the TSS region of *Prss53* upon knockdown of MafA or NCoA6, the regulatory pattern expected for MafA-recruited Mll3/4 activity (Fig. 3*D* and *E*).

Human MAFA and MAFB Interact With the MLL3/4 Complexes

Our next objective was to determine if human MAFA and closely related MAFB bind MLL3/4. MafB is produced in insulin$^+$ cells only during mouse embryogenesis and plays an important role in β-cell formation (19). In contrast, human MAFB is expressed in developing and postnatal β-cells, being coproduced with MAFA in adult islet β-cells (20). These basic leucine-zipper proteins bind to DNA with identical specificity as homo- or heterodimers (32,42),

as also observed in MAFA- and MAFB-transfected HeLa cell extracts (Fig. 4*A*). Gel shift analysis indicates that both MAFA/MAFB and $MAFB_2$ complexes are also formed in nuclear extracts prepared from the human EndoC-βH1 β-cell line (Fig. 4*B*), although they were difficult to distinguish due to their similar size (MAFA at ~45 vs. MAFB at ~42 kDa). Supershift analysis with MAFA and MAFB antibodies provided further support for these protein associations (Fig. 4*A*: lanes 3–5; Fig. 4*B*: lane 3). Significantly, immunoprecipitation experiments demonstrated that MAFA and MAFB were both able to associate with multiple proteins of the MLL3/4 complex in EndoC-βH1 cells (NCOA6, UTX, RBBP5) (Fig. 4*C*), although whether this results from binding $MAFB_2$ and/or MAFA/MAFB is unclear. In addition, MAFA and MAFB were able to interact with the islet-enriched PAX6 and ISL1 transcription factors as well as P/CAF; however, these likely represent relatively weak or indirect binding due to their absence from the Re-CLIP/MS analysis performed in mouse βTC-3 cells (Supplementary Table 1).

MAFA, MAFB, and the MLL3/4 Complexes Are Necessary for Glucose-Responsive Insulin Secretion in EndoC-βH1 Cells

MAFA, MAFB, and NCOA6 were siRNA depleted from EndoC-βH1 cells to analyze their significance to human β-cell gene expression and function. Protein levels were reduced by ~50–70% under these conditions (Fig. 5*A*). The effect on transcriptional control was determined on genes regulated by mouse MafA and a candidate set available on a commercial array composed of 84 genes associated with T2DM onset, development, and progression.

INSULIN, G6PC2, *PRSS53*, and *SLC2A1* were significantly affected by MAFA or MAFB depletion in EndoC-βH1 cells (Fig. 5*B*). However, their expression was unchanged

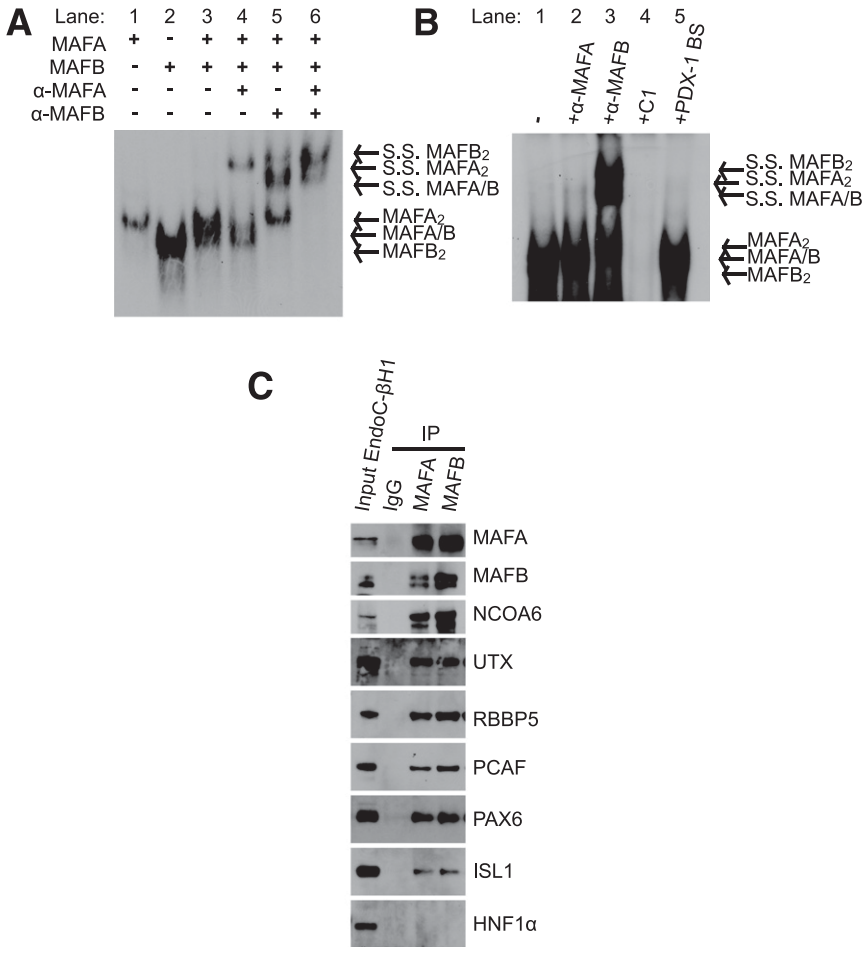

Figure 4—MAFA and MAFB associate with MLL3/4 in human EndoC-βH1 cells. *A*: $MAFA_2$, $MAFB_2$, and MAFA/B are produced in MAFA and MAFB transfected HeLa cells. Supershift (S.S.) reveals three distinct complexes, with anti-MAFA and anti-MAFB altering homo- and heterodimer formation. *B*: $MAFB_2$ and MAFA/B appear to be the predominant gel shift complexes formed in EndoC-βH1 nuclear extracts. Note that complex formation is profoundly affected by the addition of anti-MAFB. The *rat insulin II* C1 and Pdx-1 binding element competitions illustrate the specificity of complex binding. *C*: Subunits of MLL3/4 were precipitated from EndoC-βH1 nuclear extracts with antibodies to MAFA and MAFB. Immunoblotting was performed for MLL3/4 subunits (NCOA6, RBBP5, UTX), islet-enriched transcription factors (PAX6, ISL1, HNF1α), and mouse MafA associated P/CAF (18). Representative blot is shown (n = 3).

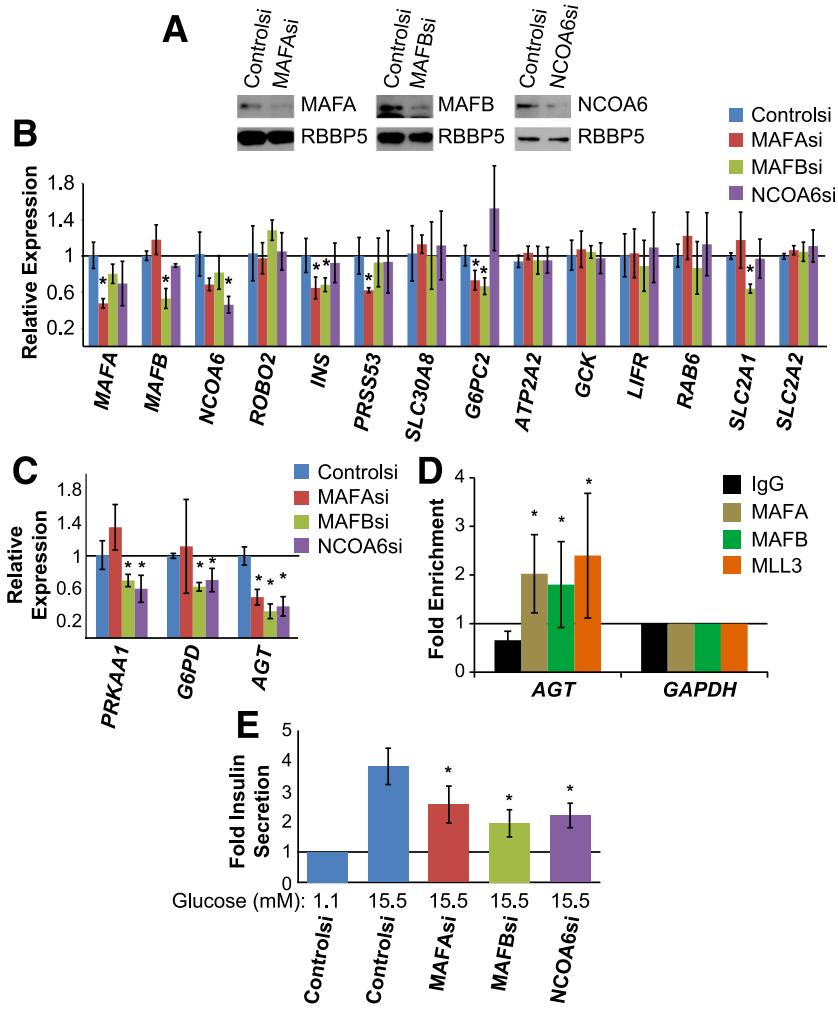

Figure 5—MAFA, MAFB, and MLL3/4 are required for glucose-stimulated insulin secretion in EndoC-βH1 cells. *A*: Protein levels of MAFA, MAFB, and NCOA6 were reduced upon targeted siRNA treatment. Densitometric analysis indicated effective knockdown of MAFA (0.44 ± 0.18), MAFB (0.53 ± 0.29), and NCOA6 (0.26 ± 0.05; $n = 3$). *$P < 0.05$. The effect of knockdown on β-cell mRNA levels was determined using bona fide MafA-activated genes of mouse β-cells (*B*) and by candidate gene screening using the Qiagen human diabetes RT^2 profiler array (*C*). qPCR results were normalized to GAPDH expression. Error bars depict the SD ($n = 4$). *D*: MAFA, MAFB, and MLL3 bind within the same region of *AGT*. Fold enrichment was calculated from the percentage input normalized to GAPDH ($n = 4$). *E*: Glucose-stimulated insulin secretion was measured 1 h after glucose stimulation in cells treated with siRNA for 72 h. Results are presented as fold stimulation at 15.5 mmol/L vs. 1.1 mmol/L glucose; all measurements were normalized for insulin content ($n = 4$). Error bars indicate the SD. *$P < 0.05$.

by NCOA6 depletion, presumably due to differences in human MAFA/MAFB:MLL3/4 control in relation to rodents and/or the β-cell lines used in our analysis. Notably, the levels of several genes linked to T2DM and important to glucose-stimulated insulin secretion were reduced upon NCOA6 depletion (Fig. 5*C*), specifically, AMP-kinase subunit *PRKAA1* (43), glucose-6-phosphate dehydrogenase (44), and angiotensin (*AGT*) (45). In addition, the expression of each was compromised in MAFB siRNA-treated EndoC-βH1 cells, whereas MAFA depletion only affected *AGT*. Moreover, MAFA, MAFB, and MLL3 were all corecruited to the same endogenous 5′-flanking control region of the *AGT* gene (Fig. 5*D*). Furthermore, glucose-stimulated insulin secretion in EndoC-βH1 cells was compromised upon knockdown of MAFA, MAFB, or NCOA6 (Fig. 5*E*). Collectively, these data support an important role for MLL3/4 in MAFA and MAFB activity in human β-cells.

Conditional Knockout of MafA or NCoA6 in Islet β-Cells In Vivo Decreases MafA Target Gene Expression and Glucose-Responsive Insulin Secretion

To evaluate the influence of MafA:Mll3/4 on islet β-cells in mice, we compared the phenotype of β-cell–specific loss of NCoA6 with that of MafA. Rat *insulin II*–driven Cre transgenic mice (30) were bred with *MafA*$^{fl/fl}$ (19) and *NCoA6*$^{fl/fl}$ (46) mice to remove these proteins specifically from insulin$^+$ cells in *MafA*$^{\Delta\beta}$ and *NCoA6*$^{\Delta\beta}$ mice during development (Fig. 6*A*). Approximately 70% of mutant insulin$^+$ cells lacked the MafA or NCoA6 proteins by e15.5 (Fig. 6*B*), a time at which MafB is still expressed in developing β-cells (47).

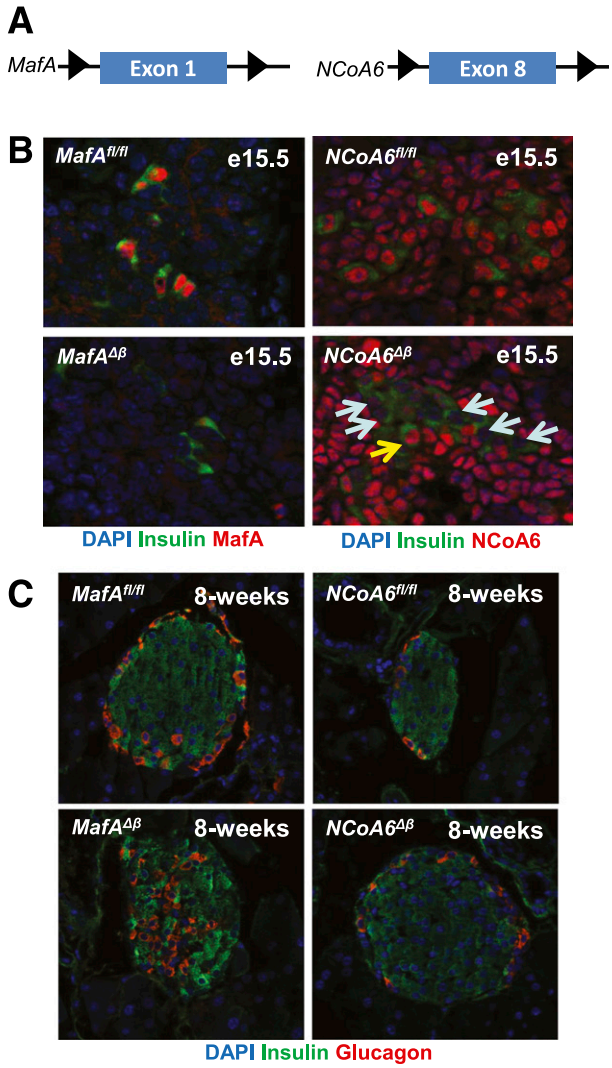

Figure 6—Islet architecture is unchanged in *NCoA6*$^{\Delta\beta}$ mice. *A*: *MafA*$^{\Delta\beta}$ and *NCoA6*$^{\Delta\beta}$ mice were generated by breeding *MafA*$^{fl/fl}$ and NCoA6$^{fl/fl}$ mice with rat *insulin II* enhancer/promoter (RIP)-driven Cre transgenic mice. The MafA protein coding sequence is only present within exon 1 (19), while deletion of exon 8 causes a frame shift that prevents the production of NCoA6 (46). *B*: Representative images illustrate the effectiveness of MafA and NCoA6 removal from insulin$^+$ cells at e15.5; ~72% of insulin$^+$ cells lack MafA or NCoA6. The blue arrows indicate insulin$^+$ cells lacking NCoA6, and the yellow arrow indicates a cell still expressing NCoA6 (n = 3). *C*: Islet architecture is only distorted in *MafA*$^{\Delta\beta}$ mice at 8 weeks.

Like the pancreas-specific *Pdx1-Cre* removal of MafA (*MafA*$^{\Delta panc}$) (41), *MafA*$^{\Delta\beta}$ mice were euglycemic and had impaired islet architecture, where glucagon$^+$ α-cells were no longer restricted to the outer mantle of the islet (Fig. 6*C*). Adult *NCoA6*$^{\Delta\beta}$ mice were also euglycemic, but their islet architecture was unchanged. In addition, only *MafA*$^{\Delta\beta}$ mice displayed the impaired whole-body glucose clearance observed in *MafA*$^{\Delta panc}$ mice (41) (Supplementary Fig. 2*B–E*).

Strikingly, most of the genes regulated by MafA in 8-week-old *MafA*$^{\Delta\beta}$ mouse islets were now also significantly compromised in 8-week-old *NCoA6*$^{\Delta\beta}$ islets (Fig. 7*A*). In addition, glucose-stimulated insulin secretion was impaired in islets isolated from both *MafA*$^{\Delta\beta}$ and *NCoA6*$^{\Delta\beta}$ mice (Fig. 7*C*), as found upon MAFA, MAFB, or NCOA6 depletion in human EndoC-βH1 cells (Fig. 5*D*). The basal insulin secretion level of *NCoA6*$^{\Delta\beta}$ islets was unusually high in relation to wild-type controls and *MafA*$^{\Delta\beta}$ (Fig. 7*C*), a sign of β-cell immaturity (48). The more penetrant Mll3/4 control properties observed in *NCoA6*$^{\Delta\beta}$ mice likely represent the combined actions of Mll3/4 on MafB activity during development and MafA postnatally.

DISCUSSION

Gene induction involves the recruitment of coregulators by enhancer-bound transcription factors such as MAFA and MAFB. These protein-bound effectors ultimately influence recruitment of the RNA polymerase II transcriptional machinery. We used an unbiased "in cell" chemical cross-linking, immunoprecipitation, and MS strategy to identify coregulators of the MafA transcription factor, an essential regulator of postnatal rodent islet β-cell proliferation and activity. Many distinct coregulator candidates were identified in our biochemical screen, and we focused on the Mll3/4 methyltransferase complex because of the established role of this coactivator in gene transcription. Our studies are consistent with a model where MLL3/4 recruitment by MAFA and MAFB is essential to islet β-cells.

MLL3 and MLL4 are members of the evolutionary-conserved COMPASS family of methyltransferases that are strongly associated with gene activation due to their ability to methylate H3K4 within enhancer and/or promoter regions. Strikingly, all of the proteins in the Mll3/4 complexes were identified in the MafA antibody precipitates by MS, and not the other mammalian Mll complexes (e.g., Mll1/2 complex or Set1A/B complex). MLL3/4 binding to MAFA was also confirmed by immunoprecipitation analysis in mouse and human β-cell lines (Figs. 2 and 4). Moreover, a significant fraction of MafA was bound to the ~1.5 MDa Mll3/4 complex by sucrose gradient centrifugation (Fig. 2). Interestingly, the islet-enriched Nkx2.2 and Nkx6.1 transcription factors were also found in the same high–molecular weight fraction. Although the identity of these islet-enriched complexes are unknown, a very high–molecular weight complex would be predicted from the association in β-cells of Nkx2.2 with the histone deacetylase-1 corepressor, the Groucho-3 transcription factor repressor, and the DNA (cytosine-5)-methyltransferase 3A corepressor to prevent expression of the α-cell specification factor Arx (49). Likewise, Pax6 comigration with MafA:Mll3/4 could reflect binding to high–molecular weight proteins like p300 (50). However, Nkx2.2, Nkx6.1, and Pax6 were not detected by MafA antibody in Re-CLIP experiments, and no other islet-enriched transcription factors were either (Supplementary Table 3), strongly suggesting that these proteins are not directly, and certainly not abundantly, associated with MafA:Mll3/4. At least some interaction is likely with PAX6 and ISL1 in human β-cells based on the MAFA and

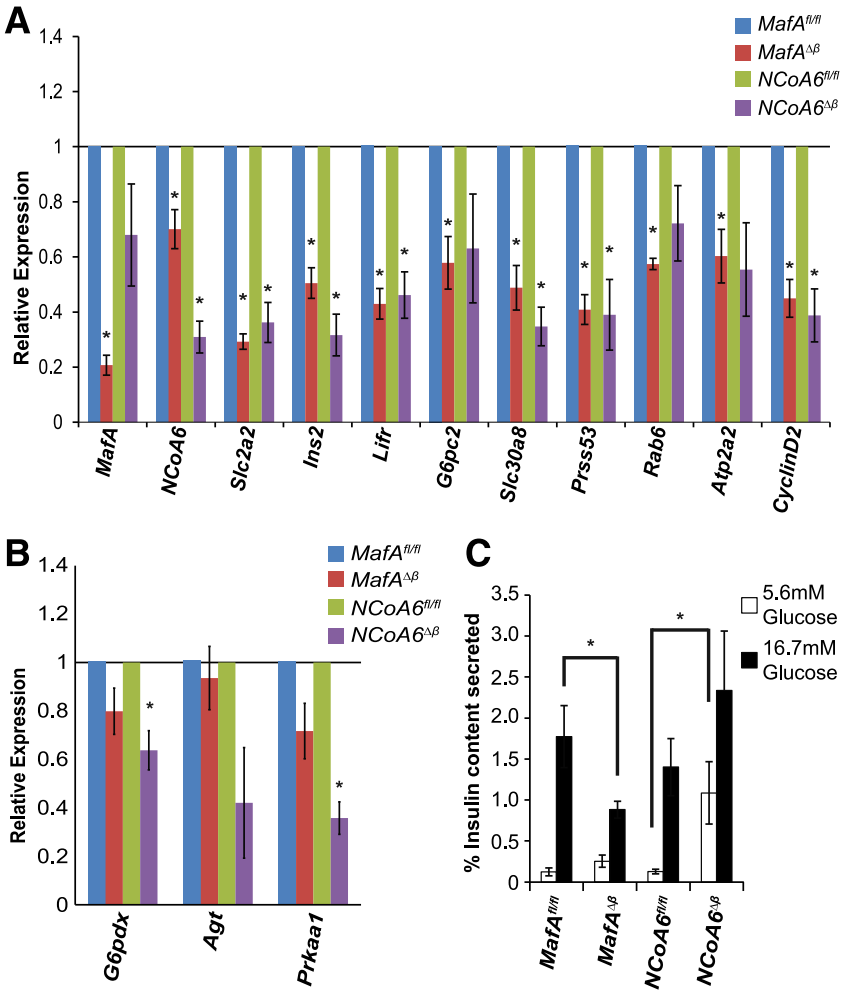

Figure 7—Glucose-stimulated insulin secretion is impaired in *MafA*$^{\Delta\beta}$ and *NCoA6*$^{\Delta\beta}$ islets. Expression of all the direct targets of mouse MafA was decreased in 8-week-old *MafA*$^{\Delta\beta}$ islets (*A*) but not those identified as human MAFA- and/or MAFB-regulated genes by Qiagen human diabetes RT^2 profiler screening (*B*) (see Fig. 5*C*). Moreover, essentially all of these genes were also compromised in *NCoA6*$^{\Delta\beta}$ islets. The error bars indicate the SEM (n = 3–5). Fold expression was normalized to control littermates. *C*: Isolated islets were incubated overnight in low glucose (5.6 mmol/L) and then treated with 5.6 mmol/L or stimulating 16.7 mmol/L glucose for 1 h. The data are presented as the percentage (%) of total insulin content secreted. The error bars represent the SEM. n for *MafA*$^{fl/fl}$ = 3, *MafA*$^{\Delta\beta}$ = 4, *NCoA6*$^{fl/fl}$ = 3, *NCoA6*$^{\Delta\beta}$ = 3. *$P < 0.05$.

MAFB antibody precipitation results in human EndoC-βH1 cells (Fig. 4*C*). Collectively, these data strongly implied that MafA recruitment of Mll3/4 was highly specific and important to β-cell activity.

Immunoprecipitation experiments conducted with the EndoC-βH1 cell line showed that human MAFA and MAFB are both capable of binding and recruiting the MLL3/4 complexes. However, reducing the protein levels of these transcription factors or the core NCOA6 subunit of the MLL3/4 complexes in human (Fig. 5) and mouse (Fig. 3) β-cell lines disclosed that the coactivator only influenced some MAFA/MAFB activated genes. For example, only the *Slc2a2* and *Prss53* genes were bound and coregulated by MafA and Mll3/4 among a variety of tested MafA-regulated genes in βTC-3 cells (Fig. 3). Importantly, and as expected, recruitment of Mll3/4 by MafA regulated H3K4 trimethylation levels of the *Prss53* gene as well as RNA polymerase II engagement.

In contrast to what was found upon reduction of NCoA6 levels in β-cell lines, nearly all of the islet MafA target genes were dependent on NCoA6 in 8-week-old *NCoA6*$^{\Delta\beta}$ islets (Fig. 7*A*). Because of the early action of Cre-recombinase in developing MafA$^+$ and MafB$^+$ *NCoA6*$^{\Delta\beta}$ β-cells, this more penetrant phenotype is likely due to the activity of Mll3/4 on MafB-bound enhancers during development. Notably, this supposition is consistent with analysis of the *MafB*$^{-/-}$ (19) and *MafA*$^{\Delta panc}$ (41) mutants, which established that many genes first regulated by MafB developmentally were subsequently influenced by MafA after birth (41). In *NCoA6*$^{\Delta\beta}$ mice, the lack of Mll3/4 activity on MafA- and MafB-bound enhancers during development may explain why glucose-stimulated insulin secretion was differentially affected in *NCoA6*$^{\Delta\beta}$ and *MafA*$^{\Delta\beta}$ islets (Fig. 7*C*). The results also indicate that Mll3/4 is involved in some, but not all, MafA- and MafB-regulated gene expression. Thus, Mll3/4 was necessary

for glucose-stimulated insulin secretion in both human and mouse β-cells but did not have the same influential effect on islet cell architecture as MafA (Fig. 7*A*).

Our understanding of the genes regulating glucose-stimulated insulin secretion in human β-cells is very limited. The results in EndoC-βH1 cells suggest that regulation by MAFA/B:MLL3/4 of the AMP-kinase subunit *PRKAA1* (43), glucose-6-phosphate dehydrogenase (44), and angiotensin (45) expression may be important (Fig. 5*C*). For example, angiotensin appears to have a direct role in regulating β-cell activity (51). However, this candidate list certainly represents only a fraction of the gene products involved in β-cell function, and future efforts will be aimed at identifying more using ChIP-Seq and RNA-Seq. This analysis should also be conducted with human islets, because the transformed and proliferative nature of the EndoC-βH1 cell line could possibly influence how MAFA and MAFB regulate gene expression. It is also important to note how similar the phenotype of the MAFA, MAFB, and NCOA6 regulatory response was in our β-cell line and mouse studies, and yet different from the other islet-enriched transcription factors present in high–molecular weight complexes (Fig. 2). Thus, islet β-cell–specific deletion of Pax6, Nkx2.2, or Nkx6.1 produces a much more severe effect on cell identity and causes lethality soon after birth due to hyperglycemia (52–54).

In conclusion, our combined proteomic, cell line, and mouse strategies have led to the identification and characterization of MLL3/4 as a novel coactivator of the MAFA and MAFB transcription factors in islet β-cells. Future efforts will be aimed at determining how other isolated candidate coregulators affect MAFA and MAFB control, such as CoREST (LSD1, RCOR1, RCOR3, HDAC2) and histone deacetylase 6, both of which are known to play a major regulatory role in other cell contexts (55,56). It will also be of interest to determine if coregulator recruitment is influenced by homodimeric (i.e., $MAFA_2$, $MAFB_2$) or heteromeric (MAFA/MAFB) transcription factor composition and the physiological or pathophysiological state of the β-cell.

Acknowledgments. Adenoviral Flag-tagged MafA was kindly provided by Dr. Qiao Zhou, Harvard University. The authors thank Dr. Raphael Scharfmann, INSERM, Paris, France, and Dr. Philippe Ravassard, French National Centre for Scientific Research, Paris, France, for generously providing EndoC-βH1 cells.

Funding. This work was supported by grants from the National Institutes of Health (DK-090570 to R.S., F32-DK-102283-01 and T32-DK-007061 to H.A.C., and CA-112403 and DK-058242 to J.X.) and the Vanderbilt Diabetes Research and Training Center (DK-20593). Imaging was performed with National Institutes of Health support from the Vanderbilt University Medical Center Cell Imaging Shared Resource (CA-68485, DK-20593, DK-58404, HD-15052, DK-59637, and EY-08126) and Vanderbilt University Medical Center Islet Procurement and Analysis Core (DK-20593).

Duality of Interest. No potential conflicts of interest relevant to this article were reported.

Author Contributions. D.W.S. and H.A.C. researched data and wrote the manuscript. L.L. and J.X. provided animals. A.R. provided technical support. S.G. researched data. R.S. wrote the manuscript. R.S. is the guarantor of this work, and, as such, had full access to all the data in the study and takes responsibility for the integrity of the data and the accuracy of the data analysis.

References

1. Mayhew CN, Wells JM. Converting human pluripotent stem cells into beta-cells: recent advances and future challenges. Curr Opin Organ Transplant 2010;15:54–60
2. Pagliuca FW, Melton DA. How to make a functional β-cell. Development 2013;140:2472–2483
3. Aguayo-Mazzucato C, Koh A, El Khattabi I, et al. Mafa expression enhances glucose-responsive insulin secretion in neonatal rat beta cells. Diabetologia 2011;54:583–593
4. Jonsson J, Carlsson L, Edlund T, Edlund H. Insulin-promoter-factor 1 is required for pancreas development in mice. Nature 1994;371:606–609
5. Stoffers DA, Zinkin NT, Stanojevic V, Clarke WL, Habener JF. Pancreatic agenesis attributable to a single nucleotide deletion in the human IPF1 gene coding sequence. Nat Genet 1997;15:106–110
6. Gradwohl G, Dierich A, LeMeur M, Guillemot F. Neurogenin3 is required for the development of the four endocrine cell lineages of the pancreas. Proc Natl Acad Sci U S A 2000;97:1607–1611
7. Nishimura W, Kondo T, Salameh T, et al. A switch from MafB to MafA expression accompanies differentiation to pancreatic beta-cells. Dev Biol 2006; 293:526–539
8. D'Amour KA, Bang AG, Eliazer S, et al. Production of pancreatic hormone-expressing endocrine cells from human embryonic stem cells. Nat Biotechnol 2006;24:1392–1401
9. Zhou Q, Brown J, Kanarek A, Rajagopal J, Melton DA. In vivo reprogramming of adult pancreatic exocrine cells to beta-cells. Nature 2008;455:627–632
10. Luo H, Chen R, Yang R, et al. Reprogramming of mice primary hepatocytes into insulin-producing cells by transfection with multicistronic vectors. J Diabetes Res 2014;2014:716163.
11. Akinci E, Banga A, Tungatt K, et al. Reprogramming of various cell types to a beta-like state by Pdx1, Ngn3 and MafA. PLoS One 2013;8:e82424
12. Millard CJ, Watson PJ, Fairall L, Schwabe JW. An evolving understanding of nuclear receptor coregulator proteins. J Mol Endocrinol 2013;51:T23–T36
13. Qiu Y, Guo M, Huang S, Stein R. Insulin gene transcription is mediated by interactions between the p300 coactivator and PDX-1, BETA2, and E47. Mol Cell Biol 2002;22:412–420
14. Ogihara T, Vanderford NL, Maier B, Stein RW, Mirmira RG. Expression and function of Set7/9 in pancreatic islets. Islets 2009;1:269–272
15. Mosley AL, Ozcan S. The pancreatic duodenal homeobox-1 protein (Pdx-1) interacts with histone deacetylases Hdac-1 and Hdac-2 on low levels of glucose. J Biol Chem 2004;279:54241–54247
16. Liu A, Desai BM, Stoffers DA. Identification of PCIF1, a POZ domain protein that inhibits PDX-1 (MODY4) transcriptional activity. Mol Cell Biol 2004;24:4372–4383
17. Stanojevic V, Yao KM, Thomas MK. The coactivator Bridge-1 increases transcriptional activation by pancreas duodenum homeobox-1 (PDX-1). Mol Cell Endocrinol 2005;237:67–74
18. Rocques N, Abou Zeid N, Sii-Felice K, et al. GSK-3-mediated phosphorylation enhances Maf-transforming activity. Mol Cell 2007;28:584–597
19. Artner I, Hang Y, Mazur M, et al. MafA and MafB regulate genes critical to beta-cells in a unique temporal manner. Diabetes 2010;59:2530–2539.
20. Dai C, Brissova M, Hang Y, et al. Islet-enriched gene expression and glucose-induced insulin secretion in human and mouse islets. Diabetologia 2012;55:707–718
21. Yeom SY, Kim GH, Kim CH, et al. Regulation of insulin secretion and beta-cell mass by activating signal cointegrator 2. Mol Cell Biol 2006;26:4553–4563
22. Zhao L, Guo M, Matsuoka TA, et al. The islet beta cell-enriched MafA activator is a key regulator of insulin gene transcription. J Biol Chem 2005;280: 11887–11894
23. Ravassard P, Hazhouz Y, Pechberty S, et al. A genetically engineered human pancreatic β cell line exhibiting glucose-inducible insulin secretion. J Clin Invest 2011;121:3589–3597

24. Matsuoka TA, Kaneto H, Stein R, et al. MafA regulates expression of genes important to islet beta-cell function. Mol Endocrinol 2007;21:2764–2774
25. Guo S, Vanderford NL, Stein R. Phosphorylation within the MafA N terminus regulates C-terminal dimerization and DNA binding. J Biol Chem 2010;285: 12655–12661
26. Smith AL, Friedman DB, Yu H, Carnahan RH, Reynolds AB. ReCLIP (reversible cross-link immuno-precipitation): an efficient method for interrogation of labile protein complexes. PLoS One 2011;6:e16206
27. Livak KJ, Schmittgen TD. Analysis of relative gene expression data using real-time quantitative PCR and the 2(-Delta Delta C(T)) method. Methods 2001;25:402–408
28. Deramaudt TB, Sachdeva MM, Wescott MP, Chen Y, Stoffers DA, Rustgi AK. The PDX1 homeodomain transcription factor negatively regulates the pancreatic ductal cell-specific keratin 19 promoter. J Biol Chem 2006;281:38385–38395
29. Kawagoe J, Li Q, Mussi P, et al. Nuclear receptor coactivator-6 attenuates uterine estrogen sensitivity to permit embryo implantation. Dev Cell 2012;23:858–865
30. Postic C, Shiota M, Niswender KD, et al. Dual roles for glucokinase in glucose homeostasis as determined by liver and pancreatic beta cell-specific gene knock-outs using Cre recombinase. J Biol Chem 1999;274:305–315
31. Stefan Y, Meda P, Neufeld M, Orci L. Stimulation of insulin secretion reveals heterogeneity of pancreatic B cells in vivo. J Clin Invest 1987;80:175–183
32. Matsuoka TA, Zhao L, Artner I, et al. Members of the large Maf transcription family regulate insulin gene transcription in islet beta cells. Mol Cell Biol 2003;23: 6049–6062
33. Völkel P, Le Faou P, Angrand PO. Interaction proteomics: characterization of protein complexes using tandem affinity purification-mass spectrometry. Biochem Soc Trans 2010;38:883–887
34. Eissenberg JC, Shilatifard A. Histone H3 lysine 4 (H3K4) methylation in development and differentiation. Dev Biol 2010;339:240–249
35. Kim DH, Lee J, Lee B, Lee JW. ASCOM controls farnesoid X receptor transactivation through its associated histone H3 lysine 4 methyltransferase activity. Mol Endocrinol 2009;23:1556–1562
36. Lee S, Lee J, Lee SK, Lee JW. Activating signal cointegrator-2 is an essential adaptor to recruit histone H3 lysine 4 methyltransferases MLL3 and MLL4 to the liver X receptors. Mol Endocrinol 2008;22:1312–1319
37. Lee J, Saha PK, Yang QH, et al. Targeted inactivation of MLL3 histone H3-Lys-4 methyltransferase activity in the mouse reveals vital roles for MLL3 in adipogenesis. Proc Natl Acad Sci U S A 2008;105:19229–19234
38. Lee S, Lee DK, Dou Y, et al. Coactivator as a target gene specificity determinant for histone H3 lysine 4 methyltransferases. Proc Natl Acad Sci U S A 2006;103:15392–15397
39. Burghardt H, López-Bermejo A, Baumgartner B, et al. The nuclear receptor coactivator AIB3 is a modulator of HOMA beta-cell function in nondiabetic children. Clin Endocrinol (Oxf) 2008;69:730–736
40. Tennant BR, Robertson AG, Kramer M, et al. Identification and analysis of murine pancreatic islet enhancers. Diabetologia 2013;56:542–552
41. Hang Y, Yamamoto T, Benninger RK, et al. The MafA transcription factor becomes essential to islet β-cells soon after birth. Diabetes 2014;63:1994–2005
42. Kerppola TK, Curran T. A conserved region adjacent to the basic domain is required for recognition of an extended DNA binding site by Maf/Nrl family proteins. Oncogene 1994;9:3149–3158
43. Sun G, Tarasov AI, McGinty J, et al. Ablation of AMP-activated protein kinase alpha1 and alpha2 from mouse pancreatic beta cells and RIP2.Cre neurons suppresses insulin release in vivo. Diabetologia 2010;53:924–936
44. Zhang Z, Liew CW, Handy DE, et al. High glucose inhibits glucose-6-phosphate dehydrogenase, leading to increased oxidative stress and beta-cell apoptosis. FASEB J 2010;24:1497–1505
45. van der Zijl NJ, Moors CC, Goossens GH, Blaak EE, Diamant M. Does interference with the renin-angiotensin system protect against diabetes? Evidence and mechanisms. Diabetes Obes Metab 2012;14:586–595
46. Wang WL, Li Q, Xu J, Cvekl A. Lens fiber cell differentiation and denucleation are disrupted through expression of the N-terminal nuclear receptor box of NCOA6 and result in p53-dependent and p53-independent apoptosis. Mol Biol Cell 2010;21:2453–2468
47. Artner I, Le Lay J, Hang Y, et al. MafB: an activator of the glucagon gene expressed in developing islet alpha- and beta-cells. Diabetes 2006;55:297–304
48. Blum B, Hrvatin SS, Schuetz C, Bonal C, Rezania A, Melton DA. Functional beta-cell maturation is marked by an increased glucose threshold and by expression of urocortin 3. Nat Biotechnol 2012;30:261–264
49. Papizan JB, Singer RA, Tschen SI, et al. Nkx2.2 repressor complex regulates islet β-cell specification and prevents β-to-α-cell reprogramming. Genes Dev 2011;25:2291–2305
50. Hussain MA, Habener JF. Glucagon gene transcription activation mediated by synergistic interactions of pax-6 and cdx-2 with the p300 co-activator. J Biol Chem 1999;274:28950–28957
51. Cole BK, Keller SR, Wu R, Carter JD, Nadler JL, Nunemaker CS. Valsartan protects pancreatic islets and adipose tissue from the inflammatory and metabolic consequences of a high-fat diet in mice. Hypertension 2010;55: 715–721
52. Ashery-Padan R, Zhou X, Marquardt T, et al. Conditional inactivation of Pax6 in the pancreas causes early onset of diabetes. Dev Biol 2004;269: 479–488
53. Du A, Hunter CS, Murray J, et al. Islet-1 is required for the maturation, proliferation, and survival of the endocrine pancreas. Diabetes 2009;58:2059–2069
54. Sander M, Sussel L, Conners J, et al. Homeobox gene Nkx6.1 lies downstream of Nkx2.2 in the major pathway of beta-cell formation in the pancreas. Development 2000;127:5533–5540
55. Qureshi IA, Gokhan S, Mehler MF. REST and CoREST are transcriptional and epigenetic regulators of seminal neural fate decisions. Cell Cycle 2010;9:4477–4486
56. Dallavalle S, Pisano C, Zunino F. Development and therapeutic impact of HDAC6-selective inhibitors. Biochem Pharmacol 2012;84:756–765